ONE MECHANISM OF HAIRPIN VORTEX GENERATION BASED ON STREAK TRANSIENT GROWTH

Y. S. Wang, C. X. Xu, W. X. Huang and G. X. Cui
Department of Engineering Mechanics, School of Aerospace
Tsinghua University
Beijing 100084, PR China
Email: xucx@tsinghua.edu.cn

ABSTRACT

The vortical structures due to the streak transient growth is studied by direct numerical simulations of the minimal channel flow at $Re_\tau = 400$. The streak profile is obtained by conditional averaging the DNS data of fully developed turbulent channel flow, in which the linearly stable streaks are prevailing. Therefore, the stable streak with moderate strength is selected and the sinuous perturbation of spanwise velocity is imposed initially. The generation of a complete hairpin vortex structure as well as the hairpin packet is observed. The mechanism for the formation of hairpin vortex is analyzed by using the vorticity transport equation along the vortex lines. The stretching and titling of the vortex lines play a significant role in the generation of the hairpin vortex.

INTRODUCTION

Coherent structures commonly exist and play significant roles in wall turbulence. Earlier flow visualization using hydrogen bubbles, dyes, or smoke (e.g. Kline *et al*., 1967; Head & Bandypoyadhyay, 1981), discovered low speed streaks and burst events in the near-wall region. Recently, the three dimensional coherent structures, i.e., hairpin or horseshoe vortex embedded in the instantaneous velocity fields were directly identified by PIV measurements (Meinhart & Adiran, 1995; Adrian *et al*., 2000; Gao *et al*., 2011) besides the evidence for the existence of hairpin vortices given by direct numerical simulations (Robinson, 1991; Zhou & Adrian, 1999; Wu & Moin, 2009). Furthermore, it was demonstrated that the hairpin vortices were also present in homogeneous shear turbulence, which is free of solid wall (Supomotsky *et al*., 2005; Vanderwel & Tavoularis, 2011).

The individual hairpin vortex was proposed by Theodorsen (1952), refers to an Ω -shaped vortical structure with two streamwise-oriented legs connected via a raised, spanwise-oriented arch. The hairpin vortices are predominant on side and appear with their heads pointing downstream and towards the high-velocity fluid (Robinson, 1991). They always formed and travelled in groups, resulting in local zones of low momentum fluid (Meinhart & Adrian, 1995; Adrian *et al*., 2000). Hairpin vortices make a major contribution to the Reynolds stresses and turbulence transport (Adrian, 2007; Lee & Sung, 2011). The scales and shapes in different time period and position away from the wall were described by Robinson (1991), Zhou *et al*. (1999) and Adrian (2007).

The near-wall cycle provided a well explanation for turbulence regeneration and sustaining in low-Reynolds number wall turbulence (Jimenez & Moin, 1991). As the Reynolds number increases, the large-scale motions in the logarithmic region become increasingly comparable in energy possession to the near-wall cycle (Balakumar & Adrian, 2007; Hutchins & Marusic, 2007). The hairpin packet is considered as an interpretation to the origin of the large-scale motion in the outer layer (Adrian, 2007). However, the mechanisms of hairpin vortex generation and their formation in groups are still lack of universal knowledge. The presently proposed mechanisms for hairpin vortex generation can be categorized into parent-offspring and instability-based scenarios. On the former scenario, Smith & Walker (1994) proposed that the parent hairpin produces localized ejections near its head and legs, and the resulting inflectional shear flow then rolls up by Kelvin-Helmholtz instability and gives birth to new hairpins. Zhou *et al*. (1999) showed that the sufficiently strong Q2 event could develop into the primary hairpin vortex and induce the following downstream, secondary and tertiary hairpin vortex, which presents a scenario of hairpin packet generation. On the latter scenario, Skote *et al*. (2002) concentrated on the streak instability and suggested that hairpin vortices are related to the varicose type perturbation, while sinuous type collision leads to streamwise vortex generation. Schoppa & Hussain (2000) found the streak can lead to spanwise 'arch' vortices generation based on sinuous instability in near-wall turbulence.

In the present study, we will present a hairpin generation mechanism based on streak sinuous instability. Using the streak profile obtained by conditional averaging the DNS data of turbulent channel flow at $Re_\tau = 400$, the generation of a complete hairpin vortex structure as well as the hairpin packet was observed. The mechanism was analyzed by using the vorticity transport equation along the vortex lines.

COMPUTATIONAL APPROACH

The linear instability of the streak and the subsequent nonlinear vortex generation are studied by direct numerical simulation of incompressible channel flow. The fully spectral algorithm is used, with periodic boundary condition in the streamwise (x) and spanwise (z) directions, and no-slip condition enforced on both walls (normal to y). Fourier expansion is employed in the x and z directions,

and Chebyshev polynomials are used in the y direction. The third-order time-splitting method is adopted for time advancement.

In the present study, the computational domain is in the minimal channel size to sustain turbulence as well as to isolate only on low-speed streak (Jimenez & Moin, 1999). For the further evolution of a hairpin vortex, the domain is three-times elongated in the streamwise direction. The friction Reynolds number is chosen to be $Re_\tau = 400$. The grids are $32 \times 192 \times 32$. For the details, see table 1.

Table 1. Computational setting

Re_τ	L_x^+	L_z^+	Δ_x^+	Δ_{ymin}^+	Δ_{ymax}^+	Δ_z^+
400	418.9	119.7	13.1	0.054	6.545	3.7

Problem Formulation

According to Schoppa & Hussain (2002), the flow field is initialized by single-side turbulent profile with a low-speed streak as the base flow.

$$U(y,z) = U_0(y) + U_s(z)g(y), \quad V = W = 0 \quad (1)$$

$$U_0(y) = \begin{cases} U_L, & y_m \leq y \leq 2\delta \\ U_T, & 0 \leq y < y_m \end{cases} \quad (2)$$

Here the $U_0(y)$ is composed of a laminar profile U_L near the upper wall and a turbulent profile U_T near the lower wall, for the detailed expression for U_L and U_T see Schoppa & Hussain (2002). Notably, the Reynolds number in present study is much higher than that of Schoppa & Hussain (2002), the related parameters to determine the distribution of $U_0(y)$ are recalculated to match the present Reynolds number $Re_\tau = 400$. The profile on the turbulent side obtained according to Eq. (2) shows good agreement with that obtained in the full-scale turbulent channel flow at the same Reynolds number. The low-speed streak is represented by $U_s(z)g(y)$, where $g(y) = y\exp(-\eta y^2)$ and η is selected to maximize $g(y)$ at $y^+ = 20$. $U_s(z)$ is the streak profile in spanwise direction, obtained by conditional average along the centre lines of the low-speed streaks at $y^+ = 20$ in the full-scale turbulent channel flow. The streak strength in $U_s(z)$ can be quantified by the maximum inclining angle of the vortex line at $y^+ = 20$ as $\theta_{20} = \tan^{-1}(|\Omega_y|_{max}/|\Omega_z|)$, where $\Omega_y = dU_s / dz$ and $\Omega_z = dU_0 / dy$. Linear stable streak with moderate strength will be chosen, to focus on the vortex generation based on streak transient growth. The streamwise-dependent spanwise velocity w' referred to as STG perturbation in Schoppa & Hussain (2002) is taken as the initial perturbation.

$$u' = v' = 0, \quad w' = A\sin(\alpha x)g(y) \quad (3)$$

Here the superscript $'$ denotes the perturbation to the two-dimensional base flow $U(y,z)$. The parameter A determines the perturbation amplitude and is set to make the initial value of $w_{rms} = 0.3$-0.5. α is the streamwise wave number, closely corresponding to the minimal x-wavelength required for turbulence sustenance (Jimenez & Moin 1999) and the maximum normal-mode growth rate.

RESULTS AND DISCUSSION

In the following, a perspective view of the individual hairpin vortex generation process will be provided first, and then vorticity transport equation along the vortex lines will be analyzed to shed some lights on dynamic mechanism for the generation of an individual hairpin vortex. The formation of hairpin packets from the evolution of an individual hairpin vortex will be shown in the domain three-times elongated in the x-direction.

A. Kinematic process of hairpin vortex generation

The kinematic process of hairpin vortex generation is divided into ten representative time instants. The flow structures including vortices and streaks at each time instants are shown in Fig. 1. The single streak (a) undergoes the initial sinuous perturbation $w'(x)$, and meanders in the z direction (b), which severs as the STG period in Schoppa & Hussain (2002). Subsequently, as the nonlinear effects become prominent, the opposite-signed streamwise vortices are generated on either side of the low speed streak (c). The streamwise vortices are advected downstream, and are stretched into two parts by the mean shear (d). The part with higher speed would catch up with the part with lower speed, which leads to partly alternative aligning of the positive and negative vortices (e). Subsequently, the stronger one would firstly form an arch-shaped structure leaning towards the weak one (f), which keep growing and bridging from the stronger side to the weaker side (g). Eventually an individual complete hairpin vortex is formed (h). But it decays in the following time (i) and breakdown into turbulence (j).

The destabilization of the normal-mode stable streak through STG mechanism has been clearly demonstrated in Schoppa & Hussain (2002). Herein, one can see that the complete hairpin vortices are generated at $t^+ = 154$, the whole process can be roughly divided into three sub-procedures: partly alternative aligning of the positive and negative vortices; the bridging process between opposite-signed streamwise vortices; formation of hairpin vortex and decaying later. In the present case, two individual hairpin vortices (asymmetric) are formed since the opposite-signed streamwise vortices providing the aligning part to each other due to the periodic condition in the streamwise direction. There is no doubt that they generate in the same routine. However, there are two points should be stressed. First, the periodic condition adopted in both x and z directions has some influences on the vortex evolution environment by providing special upstream (also downstream) disturbance to each other. In Section C, the evolution process of the streak will be studied in a three times longer domain, half of which is covered by the STG perturbation. Thus the influences of the periodic condition would be alleviated. We found that the downstream noise induced by the vortices will enhance the generation of the hairpin vortex. Second, whether all of the alternative aligning of the opposite-signed streamwise vortices would lead to the hairpin vortex generation is still an open question. The strength and spacing of the opposite-signed streamwise vortices, and the background noise would all have some kind of influence to the final formation of the hairpin vortices.

B. Dynamic process of hairpin vortex generation

Chakraborty *et al.* (2005) claimed that the vortex can be regarded as a core with finite diameter in which vorticity is concentrated. Because of the weak shear away from the wall, the vortex structures can be approximated by a bundle of vortex lines in a finite time. Therefore in the present study, the mechanism for the formation of the hairpin vortex will be investigated by analyzing the vorticity transport equation along the vortex lines.

The governing equation for vorticity vector $\boldsymbol{\omega} = \nabla \times \mathbf{V}$ can be written as (Panton 2001)

$$\frac{D\boldsymbol{\omega}}{Dt} = \boldsymbol{\omega} \cdot \mathbf{S} + \nu \nabla^2 \boldsymbol{\omega} , \qquad (4)$$

where $\mathbf{S}$ is the strain rate tensor, and $\boldsymbol{\omega} \cdot \mathbf{S}$ is the strain vector acting on the plane normal to $\boldsymbol{\omega}$. It can be decomposed as $\omega(S_{\omega\omega}\mathbf{e}_\omega + S_{\omega\tau}\mathbf{e}_\tau)$, where $\mathbf{e}_\omega = \boldsymbol{\omega} / \omega$, $\mathbf{S}_\omega = \mathbf{e}_\omega \cdot \mathbf{S}$, $S_{\omega\omega} = \mathbf{S}_\omega \cdot \mathbf{e}_\omega$, and $S_{\omega\tau} = (\mathbf{S}_\omega - S_{\omega\omega}\mathbf{e}_\omega) \cdot \mathbf{e}_\tau$. The terms of $\omega S_{\omega\omega}$ and $\omega S_{\omega\tau}$ represent the contributions to $\boldsymbol{\omega}$ from stretching and turning of $\boldsymbol{\omega}$, respectively. The viscous term on the right-hand side is negligible in the vortex growing process. Therefore, the change of the vorticity would only depend on the strain vector. As shown in Fig. 2, the vortex line between the SP (streamwise vortex with positive streamwise vorticity) and SN (streamwise vortex with negative streamwise vorticity) undergoes strong positive stretching, which leads to the sharp increase of the vorticity. At the same time, the turning effect is dominant on both sides so that the spanwise spacing of the vortex line keeps increasing (Fig. 2a). At $t^+ = 128$, the arch vortex is formed at the lifted downstream end of the strong streamwise vortex, and becomes a relative small positive stretching while the other side keeps increasing moderately. The turning term decreases but it is large enough to separate SP and SN away from each other. Compare to the previous stage, the vortex structure moves further away from the wall. At $t^+ = 154$, the hairpin vortex is formed with relatively small stretching, indicating the end of the generating process. Noteworthy, the stretching term becomes negative at the neck region, which probably accounts for the following vortex decay and breakdown.

The transport of vorticity vector along the vortex line in the vortex core reveals the mechanism of hairpin vortex generation corresponding to the three steps mentioned above. According to the stretching and turning values combined with the direction of the strain vector, the trend of the vortex development can be well predicted. It is clear that the increase of the strength of the vortex is due to the large positive stretching effect, while the spatial growing of the vortex is mainly caused by the turning effect.

C. Formation of hairpin packets

In the above, the formation of the individual hairpin vortex has been described from the kinematic and dynamic viewpoints. Notably, the periodic condition in the streamwise direction allows for the generation of two individual hairpin vortices. However, the further evolution of the generated hairpins is strongly limited by the size of the minimal channel. In order to give a sufficient space for the generated hairpin vortex evolving, the channel is three times elongated in the streamwise direction. All the computational settings keep unchanged except that the initial perturbation is only imposed in one half of the domain as used in section A, while the streak covers the whole streamwise length of the domian. Notably, it is common in the fully developed wall turbulence that the low-speed streak can be as long as one thousand wall units, and the STG perturbation imposed on the streak also agrees with the scenario in real wall turbulence (for details see Schoppa & Hussain 2002).

Figure 3 shows the whole process for hairpin packets generation, including the spanwise meandering of the low-speed streak, the formation of the primary hairpin vortex, the generation of the downstream, the secondary and the tertiary hairpin vortex. The mechanism is similar to that proposed by Zhou & Adrian (1999). However, the environment for the evolution of the primary hairpin is more complicated than that in Zhou & Adrian (1999). We started the simulation with a low-speed streak rather than only a single hairpin-like vortical structure. The STG perturbation leads to the generation of primary hairpin vortex as well as other flow structures (i.e. streamwise vortcies). Moreover, some arch-like vortices also form during the hairpin packet generation. It is interesting to note that if the initial STG perturbation $w'(x)$ is not large enough, the primary hairpin vortex would decay and no hairpin packets can be formed. This is similar to the conclusions of Zhou & Adrian (1999), which showed that only the sufficient strong initial Q2 event can lead to a hairpin packet generation. Though the result obtained here has somewhat different from that of Zhou & Adrian (1999), it can be inferred that the Parent-Offspring mechanism works once a strong enough hairpin vortex is formed.

CONCLUSION

Herein, we present a complete evolution process of the hairpin vortex generation based on streak transient growth. The kinematic process as well as the dynamic process is discussed, the main conclusions can be summarized in the following: First, the normal-mode stable streaks are still dominated in a moderate Reynolds number turbulent channel flow ($Re_\tau = 400$), indicating the STG mechanism still dominates the streak destabilization. Second, the hairpin vortex can be generated from streamwise vortices, which are the direct products of the streak transient growth under sinuous perturbations. Since the streamwise vortices commonly exist in the near-wall region of the wall-bounded turbulent flows, this mechanism is a reasonable explanation for the hairpin vortex formation in real wall turbulence. Third, in the generation of the hairpin vortex, the stretching and the turning of the vortex line are responsible for the strength increasing and spatial growing of the vortical structures, respectively. The eventual decaying and breakdown of the hairpin vortex may caused by the negative stretching. Forth, the Parent-Offspring process could be observed once the primary hairpin vortex is formed.

3

REFERENCES

Adrian, R. J., Meinhart, C. D. and Tomkins, C. D., 2000, "Vortex organization in the outer region of the turbulent boundary layer", *J. Fluid Mech.*, vol. 422, pp. 1-54.

Adrian, R. J., 2007, "Hairpin vortex organization in wall turbulence", *Phys. Fluid,* 19, 041301.

Balakumar, B. J. and Adrian, R. J., 2007, "Large- and very-large-scale motions in channel and boundary-layer flows", *Phil. Trans. R. Soc. A,* vol. 265, pp. 665-681.

Chakraborty, P., Balachandar, S. and Adrian, R. J., 2005, "On the relationships between local vortex identification schemes", *J. Fluid Mech.,* vol. 535, pp. 189-214.

Gao, Q., Ortiz-Duenas C. and Longmire. E. K., 2011, "Analysis of vortex populations in turbulent wall-bounded flows", *J. Fluid Mech.*, vol. 678, pp. 87-123.

Head, M. R. and Bandyopadhyay, P., 1981, "New aspects of turbulent boundary-layer structure", *J. Fluid Mech.*, vol. 107, pp. 297-338.

Hutchins, N. and Marusic, I., 2007, "Evidence of very long meandering features in the logarithmic region of turbulent boundary layers", *J. Fluid Mech.,* Vol. 579, pp. 1-28.

Jimenez, J. and Moin, P., 1991, "The minimal flow unit in near-wall turbulence", *J. Fluid Mech.*, vol. 225, pp. 213.

Jimenez, J. and Pinelli, A. 1999, "The autonomous cycle of near-wall turbulence", *J. Fluid Mech.,* vol. 389, no. 335-359.

Kline, SJ, Reynolds, WC, Schraub, FA and Runstadler, PW, 1967, "The structure of turbulent boundary layers", *J. Fluid Mech.*, vol. 30, pp. 741-73.

Lee, J. H. and Sung, H. J., 2011, "Very-large-scale motions in a turbulent boundary layer", *J. Fluid Mech.*, vol. 673, pp. 80-120.

Meinhart, C. and Adrian, R. J., 1995, "On the existence of uniform momentum zones in a turbulent boundary layer", *Phys. Fluid*, vol.7, no.4, pp. 694-696.

Panton, R. L., 2001, "Overview of the self-sustaining mechanisms of wall turbulence", *Progress in Aerospace Sciences*, vol. 37, no. 341-383.

Robinson, W., 1991, "Coherent motions in the turbulent boundary layer", *Annu.Rev.Fluid Mech.,* Vol. 23, pp. 601.

Schoppa, W. and Hussain, F., 2000, "Coherent structure dynamics in neal-wall turbulence", *Fluid Dynamics Research,* vol. 26 pp. 119-139.

Schoppa, W. and Hussain, F., 2002, "Coherent structure generation in near-wall turbulence", *J. Fluid Mech.*, vol. 453, pp. 57-108.

Skote, M., Haritonidis, J. H. and Henningson, D. S., 2002, "Varicose instabilities in turbulent boundary layers", *Phys. Fluid,* vol. 14, no. 7.

Smith, C. R. and Walker, J. D. A., 1994, "Turbulent wall-layer vortices", *In Fluid Vortices, Springer.*

Suponitsky, V., Cohen, J. and Bar-Yoseph, P. Z., 2005, "The generation of streaks and hairpin vortices from a localized vortex disturbance embedded in unbounded uniform shear flow", *J. Fluid Mech.*, vol. 535, pp. 65-100.

Theodorsen, T., 1952, "Mechanism of turbulence", *Proceedings of the second Midwestern Conference on Fluid Mechanics, Ohio State University*, P.1-18.

Vanderwel, C. and Tavoularis, S., 2011, "Coherent structures in uniformly sheared turbulent flow", *J. Fluid Mech.*, vol. 689, pp. 434-464.

Wu, X. H. and Moin, P., 2009, "Forest of hairpins in a low-Reynolds-number zero-pressure-gradient flat-plate boundary layer", *Phys. Fluid*, 21, 091106.

Zhou, J., Adrian, R. J., Balachandar, S. and Kendall, T. M., 1999, "Mechanisms for generating coherent packets of hairpin vortices in channel flow", *J. Fluid Mech.*, vol. 387, pp. 353-396.
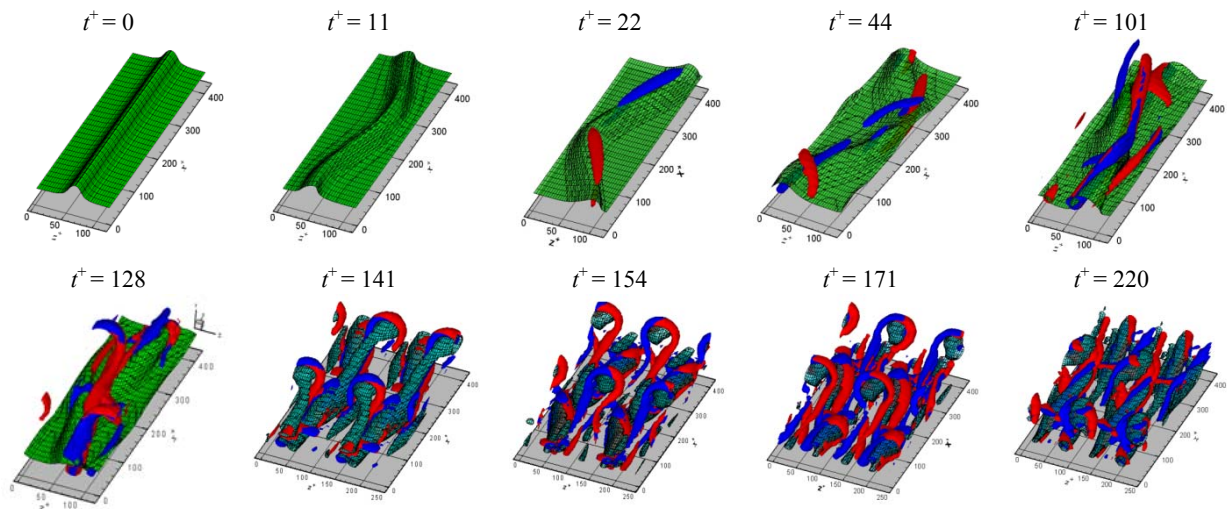
Figure 1. Time evolution of streak and vortex. The meshed surface denotes isosurface of $u = 0.5U_0$ in (a~f) and $u' = -0.1U_{mean}$ in (g~i). The domain is periodically extended in spanwise direction in (g~i). The vortex structures are shown by the isosurfaces of $\lambda_{ci} = 10$, red and blue denote positive and negative ω_x respectively

$(a)\, t^+ = 101$
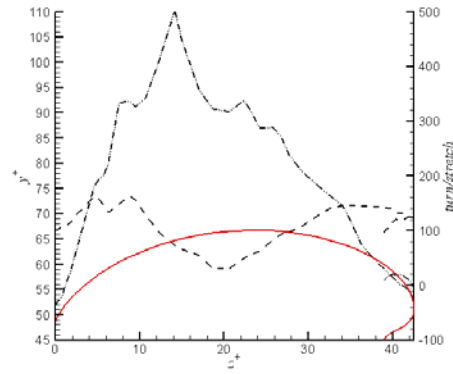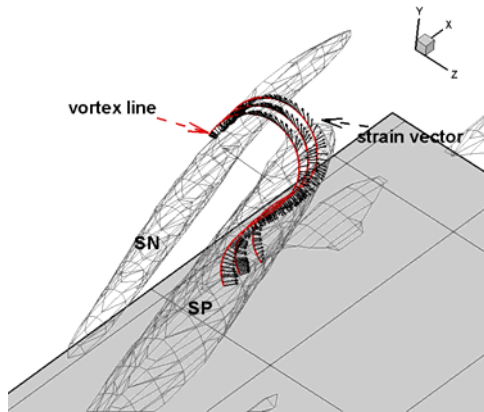
$(b)\, t^+ = 128$
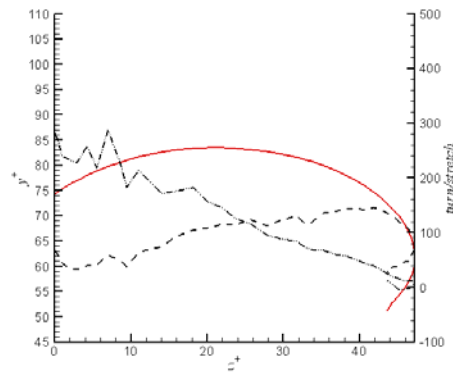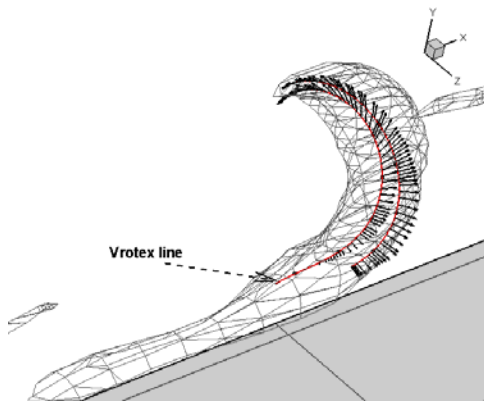
$(c)\, t^+ = 154$
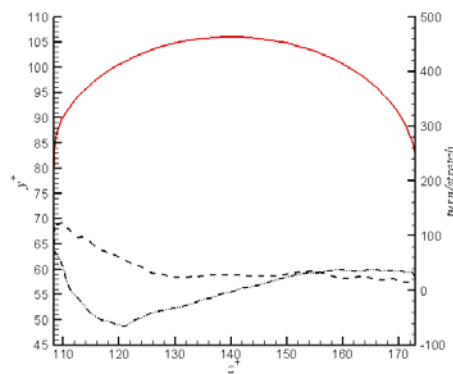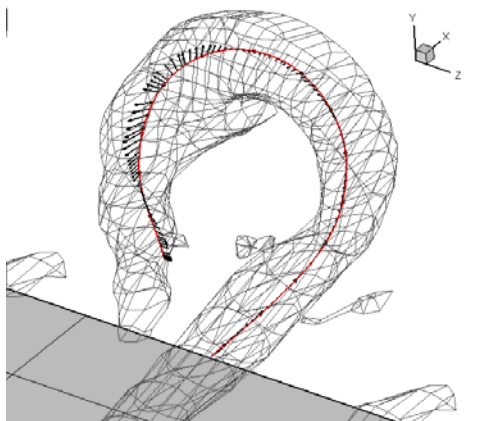
Figure 2. Stretching and turning terms acting on the vortex line at three different time instants. Left: Perspective view of the vortices and the strain vectors; Right: distribution of the stretching and turning terms along the vortex line projected to y-z plane. Meshed surface: $\lambda_{ci} = 10$; Red solid line: vortex line; Black vector: strain vector; Dashed line: turning; Dash-dotted line: stretching.
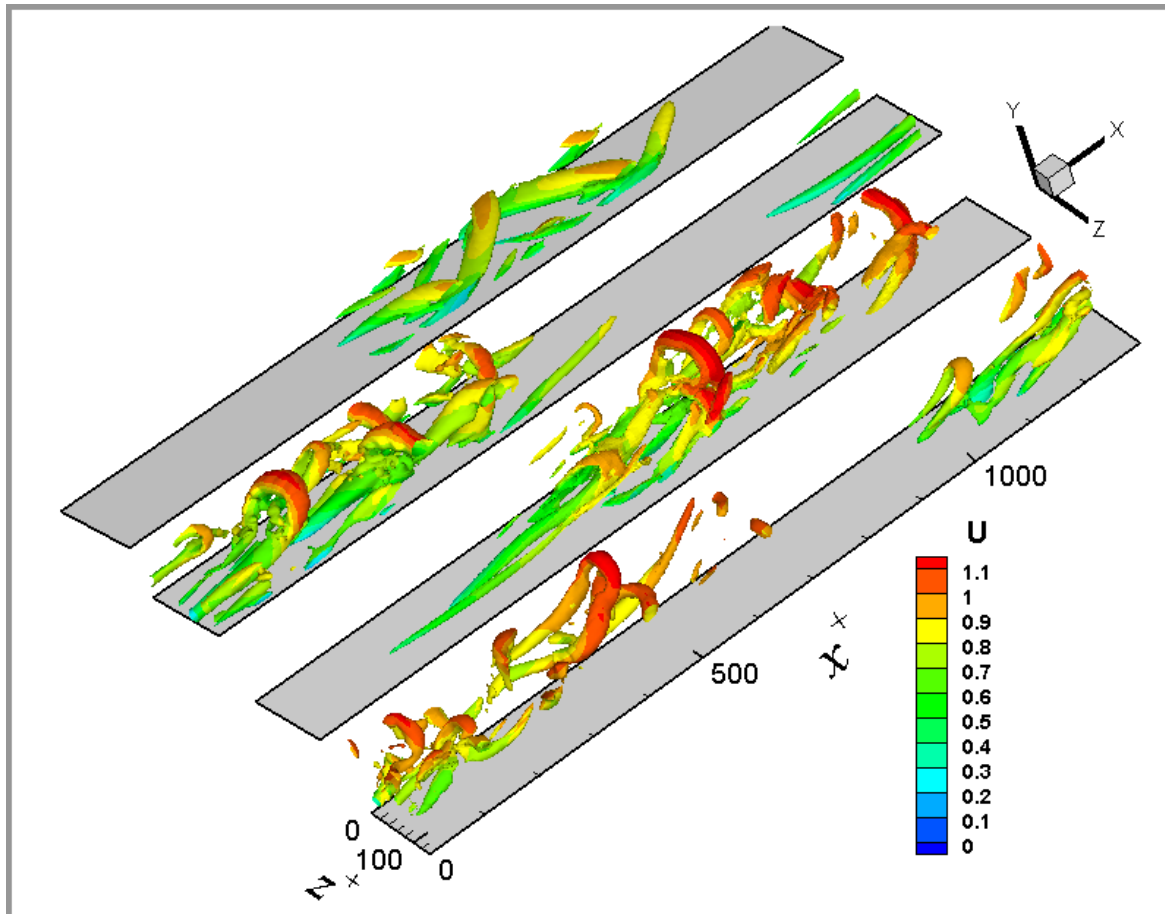
Figure 3. Perspective view of vortical structures shown by the isosurface of $\lambda_{ci} = 10$ and flooded by the streamwise velocity at $t^+ = 11, 80, 114$ and 160.